

## Spatial Electron Temperature Profile of ECH Plasma with Internal Transport Barrier on CHS

T.Minami, A.Fujisawa, H.Iguchi, S.Lee<sup>1)</sup>, Y.Yoshimura, S.Kado, K.Ida,  
K.Tanaka, K.Matsuoka, S.Okamura, M.Isobe, S.Nishimura, C.Takahashi,  
and CHS Group

*National Institute for Fusion Science, 322-6 Oroshi, Toki, Gifu 509-5292, Japan*

*1) Japan Atomic Energy Research Institute, Naka Fusion Research Establishment, Nakamachi, Naka-gun, Ibaraki, 311-0193, Japan*

### 1. Introduction

A formation of internal transport barrier (ITB) has been observed in many tokamak devices such as TFTR [1,2], DIII-D [3], and JT-60 [4]. The characteristic of the profile with the ITB is an existence of a steep gradient. Recently, a similar electron temperature profile to it has been observed in high temperature electron cyclotron heated (ECH) plasma with YAG Thomson scattering measurement [5] on CHS Heliotron/Torsatron device ( $R=1.0\text{m}$ ,  $a=0.2\text{m}$ ) [6]. In this paper, the characteristics of high temperature ECH plasma with ITB are first described. Secondly, we provide results of the YAG Thomson scattering measurement using six wavelength channel polychromator. Thirdly results of transport analysis are provided. Finally, a density threshold of the transition is described.

### 2. Electron temperature profile of ECH plasma with Internal transport barrier

Profiles of electron temperature and density were measured with a multipoint YAG Thomson scattering system [5] (24 spatial channels, 10 ms time resolution). Scattering light from low density ECH plasmas is too weak to calculate a value of the temperature and the density. Therefore, we superposed the scattering lights of 5-20 shots. A reproducibility of the shots was confirmed by line integral density with HCN interferometer and stored energy with diamagnetic measurement.

Fig. 1 (a) shows a typical electron temperature profile of ECH plasma with the ITB. The plasma is produced by a gyrotron of which frequency is 53.2 GHz. A second harmonic resonance is exactly on axis ( $B_T = 0.88\text{ T}$ ). The injected gyrotron power is  $\sim 200\text{kW}$ . The central electron temperature is  $2.2 \pm 0.1\text{ keV}$  from the 15 superposed shots. The electron density profile has a flat or slightly hollow shape and the central density is  $\sim 4 \times 10^{12}\text{ cm}^{-3}$ . Therefore, the steep pressure gradient exists at  $r/a \sim 0.3$ . These profiles indicate that the ITB is created. The gradient of the temperature at the ITB is  $0.43\text{ keV/cm}$ . For convenience, the plasma which has ITB and high electron temperature is termed high electron temperature mode (HET mode), the plasma which has no ITB is termed L mode. We compare the electron temperature profile of the HET mode to the L mode. One condition of the forming ITB is the injected ECH power. When the injected power is low ( $\sim 150\text{kW}$ ), the measured electron temperature profile has no ITB, as shown in Fig. 1 (d). The central electron temperature ( $1.3 \pm 0.1\text{ keV}$ ) is almost half of the former case.

The HIBP measurements of electric field and density fluctuation are available in  $B_T=0.88\text{T}$  [6]. The potential profile of the ECH plasma has a similar shape to the electron temperature profile, as shown in Fig. 1 (b). A rather strong  $E_r$  shear at the barrier location is deduced, whose value is approximately  $40\text{V/cm}^2$ . It is also particularly notified that the reduction in the density fluctuation level by 40% is observed, compared to the level of the case without the transport barrier. The location of the steep electron temperature gradient coincides with the location of the maximum  $E_r$  shear. The fluctuation suppression reduces the anomalous transport at the transport barrier. In the L mode case, the potential profile has no strong  $E_r$  shear, so that there is no ITB, as shown in Fig. 1 (e).

There is no density gradient at the location of the ITB, as shown in Fig.1 (c). This reason is that because of off-diagonal terms for neoclassical particle flux, a decrease in the fluctuation-driven particle flux compensates an increase in the neoclassical flux of the electron temperature gradient.

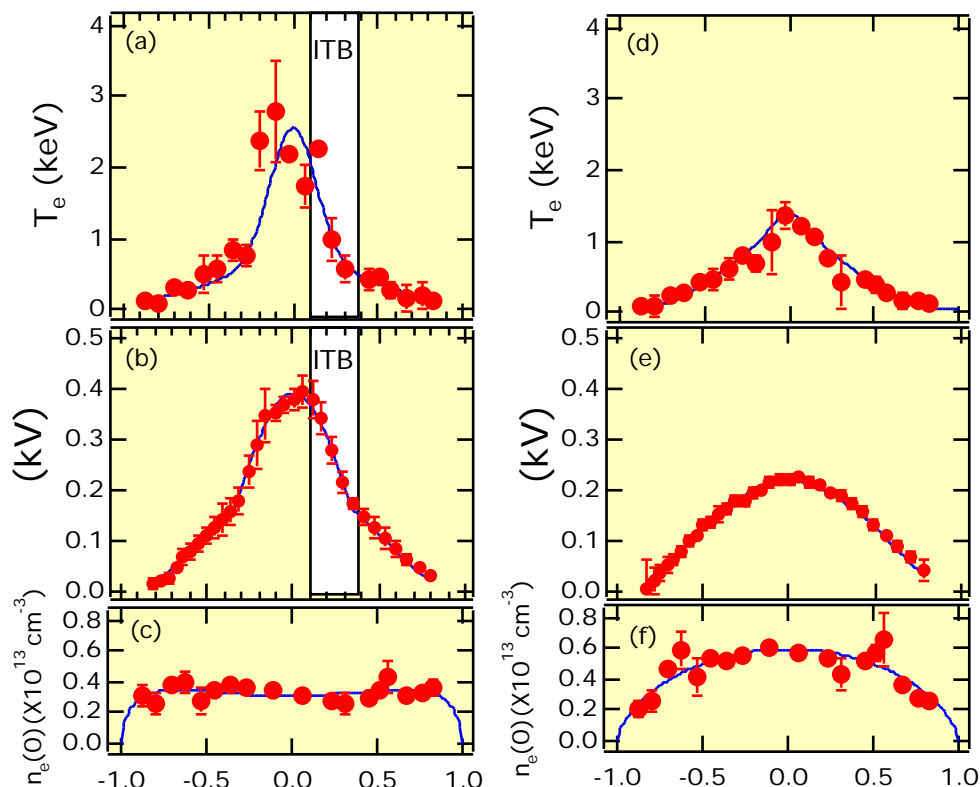


FIG.1 (a), (d) Electron temperature profile with YAG Thomson measurement. (b), (e) Potential profile of ECH plasma with HIBP. (c), (f) Electron density profile. (a), (b), (c) Injected power is  $\sim 200\text{kW}$ . Profile has ITB. (d), (e), (f) Injected power is  $\sim 150\text{kW}$ . Profile has no ITB.

### 3. Thomson spectrum shape

There is a problem whether the measured electron temperature is affected by the tail component of the electron or not. If the measured temperature is affected by the high energy electron, the temperature of the bulk electron is lower than the measured temperature. Because our Thomson scattering system has normally three wave length channels, additional channels are needed to estimate the effect of superthermal electron. However, it is not easy to modify the optical configuration of the polychromator. To solve this problem, we set a combination of center wavelength of the interference filter of polychromator to the following. (1) 570nm, 740nm, 1045nm, (2) 740nm, 840nm, 1045nm, (3) 940nm, 1000nm, 1045nm. The 1045 nm filters are used for the relative calibration of sensitivity for the three polychromators. Using these three polychromators, we can measure the Thomson scattering light at six kinds of center wavelength. The range of temperature which can be measured expands from 50 eV - 3 keV to 50 eV - 20 keV. On the other hand, spatial resolution is reduced to  $\sim 5$  cm from  $\sim 1.5$  cm, which is about half of radius of the inside region of the ITB

Fig. 2 shows Thomson scattering spectrum shape measured with the six channel polychromator. The horizontal axis indicates a square of wave length shift normalized by the YAG wave length, and the vertical axis indicates a logarithm of the intensity of the scattering light. If the measurement is affected by the high energy electrons, they have nonlinear  $I$  relation, so that the Thomson scattering spectrum shape is not gaussian. Fig. 2 (a) shows the

HET mode case. The relation of them is linear within the ITB except the point of the largest shifted wavelength, so that the Thomson scattering spectrum shape is almost gaussian. We conclude that the effect of tail electron to the calculated temperature is negligible.

The results of the six channel measurement also show that there is obvious difference of the gradient of the spectrum between the inside and the outside of the ITB as shown in Fig. 2 (a), while the difference is small in the case of L mode, as shown in Fig. 2 (b). The calculated temperature within the ITB in the HET mode case is three times as large as that of the outside region near the ITB, and is almost two times as large as that at the plasma center in the L mode case.

These clearly show the existence of the high temperature electrons within the ITB.

#### 4. Transport Analysis for ECH plasma with Internal transport barrier

To investigate the heat transport characteristic of the ITB, we carry out 1-D heat transport analysis with profile analysis code PROCTR-MOD [7]. For the calculation we used the electron temperature and density profile from YAG Thomson measurement, which is shown in Fig.1 We used a typical ion temperature profile of ECH plasma which is measured with a charge exchange spectroscopy by a diagnostic NBI. In this experiment, almost all of the ECH power is absorbed at plasma center. Fig. 3 shows electron thermal diffusivity,  $e$ , for the HET mode plasma. In the HET mode case, the electron thermal diffusivity has remarkably dropped at the transport barrier which coincides the large  $E_r$  shear region, while there is no drop in the L mode. The electron thermal diffusivity at the ITB is  $\sim 3 \text{ m}^2/\text{s}$ , which almost coincide with the diffusivity of neoclassical transport.

#### 5. Density dependence of ECH plasma with Internal transport barrier

Fig.4 shows electron temperature as a function of central electron density. In this case, the injected power is  $\sim 120 \text{ kW}$ , the  $B_T$  is 0.88 T, and the frequency is 53.2GHz. At the low density regime ( $< 5.5 \times 10^{12} \text{ cm}^{-3}$ ), as the density decreases, the central electron temperature is steeply increased from threshold density ( $\sim 4.5 \times 10^{12} \text{ cm}^{-3}$ ), while the temperature out of ITB

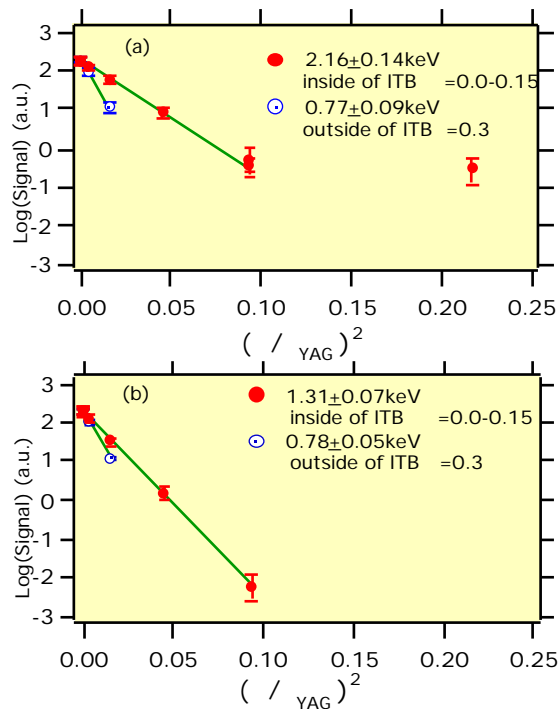


FIG.2 The Thomson scattering spectrum shape. (a) the injected power is  $\sim 200 \text{ kW}$ . Profile has ITB. (b) the injected power is  $\sim 150 \text{ kW}$ . Profile has no ITB. The horizontal axis indicates a square of wave length shift normalized by the YAG wave length, and the vertical axis indicates logarithm of the intensity of the scattering light.

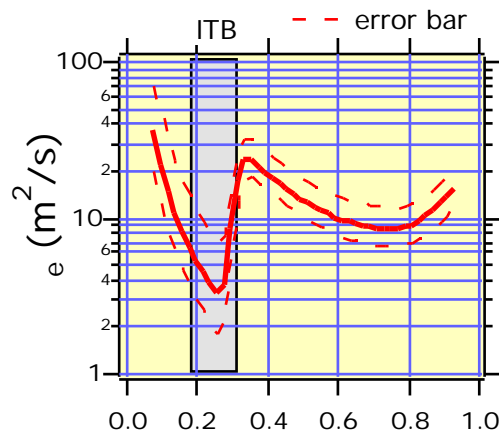


FIG.3 Radial profile of electron thermal diffusivity of ECH plasma with ITB. The broken line indicated error bar.

is gradually increased. There is no plasma with ITB at the high density regime ( $>5.5 \times 10^{12} \text{ cm}^{-3}$ ), while at the low density regime ( $<3.5 \times 10^{12} \text{ cm}^{-3}$ ), all plasma has the ITB. In the middle density regime, both type plasmas exist, whose temperature is clearly separated into two groups. These characteristics indicate that the phenomena have bifurcation nature.

As previously stated, the threshold density depends on the injected ECH power. It also depends on the magnetic field strength. We can make high density ECH plasma with the ITB at  $B_T=1.76\text{T}$  by the two methods. (1) second harmonic heating (106GHz) (2) fundamental harmonic heating (53GHz). In the first method, injected power is 250 kW, the central temperature is 1.9 keV, the gradient of the temperature at the ITB is 0.15 keV/cm, and an achieved central density is  $\sim 9 \times 10^{12} \text{ cm}^{-3}$ . In the second method, injected power is 180 kW, the central temperature is 1.8 keV, the gradient of the temperature at the ITB is 0.25 keV/cm, and an achieved central density is  $\sim 8 \times 10^{12} \text{ cm}^{-3}$ . These results indicate that the threshold density is increased by the magnetic field strength and the injected power. A duration of the ITB is determined by a duration of the ECH injection. In low injected power ( $\sim 120 \text{ kW}$ ) and lower electron density ( $\sim 3 \times 10^{12} \text{ cm}^{-3}$ ) case, we can sustain the ECH plasma with the ITB during  $\sim 100 \text{ ms}$  that is limited by the gyrotron pulse length. In this case, the central electron temperature is 1.5 - 2 keV.

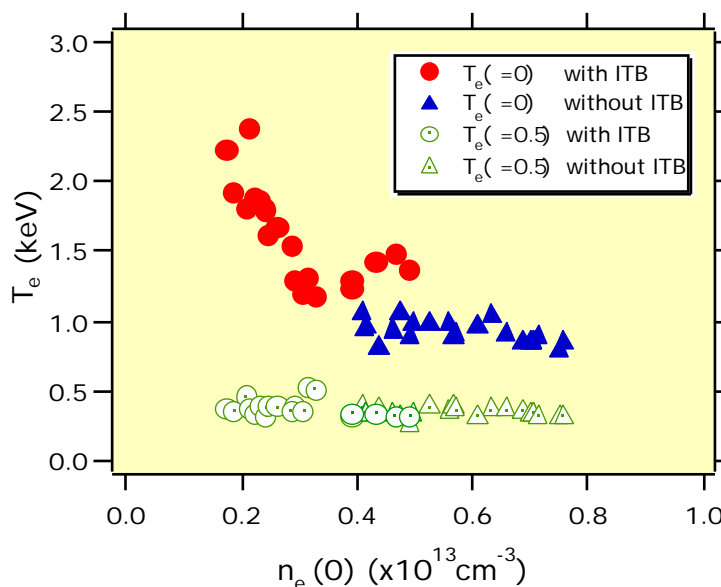


FIG.4 The electron temperature of ECH plasma as a function of central electron density. The  $P_{inj} \sim 120 \text{ kW}$ ,  $B_T = 0.88\text{T}$ , and the frequency is 53.2GHz.

## 6. Conclusions

The YAG Thomson scattering measurement of the ECH plasma of the HET mode indicates the existence of the ITB on CHS. There are high temperature electrons in the inside of the transport barrier. We have confirmed this temperature is bulk temperature using 6 channel wavelength polychromator. The transport analysis also obviously shows the existence of the ITB at the large Er shear region. The density dependence of the ECH plasma indicates that there is threshold density ( $\sim 4.5 \times 10^{12} \text{ cm}^{-3}$ ,  $P_{inj} \sim 120 \text{ kW}$ ,  $B_T = 0.88 \text{ T}$ ) at which the ITB is formed. These phenomena have bifurcation nature.

## References

- [1] F.M.Levinton, et.al., Phys.Rev.Lett 75 (1995) 4417
- [2] R.E.Bell, et.al., Plasma Phys. Control. Fusion, 40 (1998) 609
- [3] E.J.Strait, et.al., Phys.Rev.Lett 75 (1995) 4421
- [4] T.Fujita, et.al. Phys.Rev.Lett 78 (1997) 2377
- [5] K.Narihara, et.al. Rev.Sci.Instrum. 66 (9) (1995)
- [6] A.Fujisawa, et.al. Phys.Rev.Lett 82 (1999) 2669
- [7] H. C. Howe, Rep. ORNL/TM-11521, TN(1990)